VAM: hypocycloid mechanism for efficient bio-inspired robotic gaits

Espen Knoop, Andrew Conn and Jonathan Rossiter

***Abstract*— We present VAMOS (Variable Amplitude Module Orthogonal Slider), a novel two-motor hexapedal robot that is able to walk and turn with arbitrary curvature. The VAMOS walking mechanism is based around a Variable Amplitude Module (VAM), a compact and modular gearbox that produces reciprocating sinusoidal output of continuously variable amplitude. The inputs to the VAM are a drive motor, rotating at a constant speed, and a single control input for changing the output amplitude. Unlike other methods for amplitude modulation, the VAM does not require modulation of the main drive input and we can therefore operate it at peak efficiency thoughout the gait cycle. As demonstrated by VAMOS, the VAM provides a versatile building block for biomimetic robotic gaits.**

***Index Terms* — Mechanism Design of Mobile Robots, Multi-legged Robots, Hexapod, Gait Modulation, Biologically-Inspired Robots.**

I. INTRODUCTION

Nature has evolved a series of highly optimised gaits and locomotion methods, all of which rely on natural muscles for actuation. The same muscles function as motors, brakes, springs and struts [1], all of which allow for robust and energy-efficient walking, running, swimming or flying. In essence, all of these gaits can be considered as some repeated oscillatory motion. By modulating parameters such as limb trajectory, stroke length, frequency and force, the resulting overall motion is controlled.

There are a number of examples in the robotics and biomimetics literature of robots mimicking locomotion mechanisms found in Nature [2], including flying [3], swimming [4] and walking [5], [6], [7], [8]. Compared to wheeled robots, legs offer the potential for enhanced performance over rough and uneven ground. Mimicking gaits found in Nature can offer new insights to biologists about underlying principles and mechanisms. Legged robots also have a number of applications in animatronics and entertainment.

To create robots that move like their biological counterparts, we must achieve some of the functionality of natural muscle using the actuation technologies that are available to us. Robots today generally employ either pneumatic/hydraulic actuators or electric motors. Artificial Muscle technologies offer the potential of mimicking properties of natural muscle, but although significant advances have been made over the last decade (e.g. [9]) there are still a number of technological challenges that must be overcome before they can be exploited on a large scale in robotics.

EK is with Disney Research Zurich, Stampfenbachstrasse 48, 8006 Zurich, Switzerland. He carried out this work while he was a PhD student at (1) and (2). AC is with (1) and (3). JR is with (1) and (2). (1): Soft Robotics Group, Bristol Robotics Laboratory, UK. (2): Dept. Engineering Mathematics, University of Bristol, UK. (3): Dept. Mechanical Engineering, University of Bristol, UK. espen.knoop@disneyresearch.com

EK was funded by a James Dyson Foundation PhD scholarship. JR was supported by the Engineering and Physical Sciences Research Council (EPSRC) though grants EP/M020460/1 and EP/M026388/1. JR and AC were supported by RoboSoft, the FP7 Coordination Action on Soft Robotics.

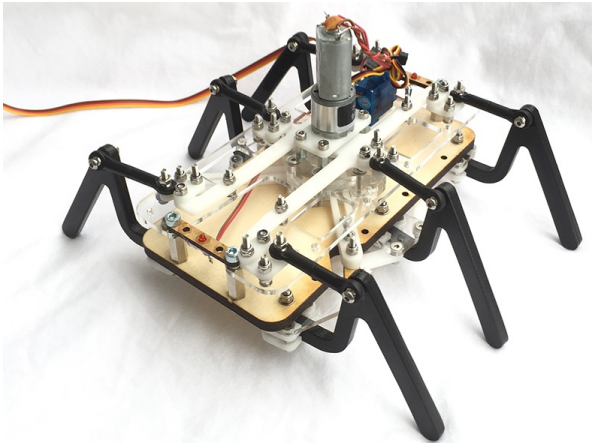

Fig. 1. The VAMOS: Variable Amplitude Module Orthogonal Slider

A widely adopted approach in legged robotics is to employ one actuator per joint. While this allows for each joint to be independently controlled, thus enabling any gait, the implementation is mechanically relatively complex and distally located actuators increase limb moment of inertia. Actuators must withstand high loads, and the gait must also be driven entirely by the central controller. It is desirable to create walking robots using less than one actuator per joint. Fundamental to any walking robot is the ability to control the gait, for example to enable turning.

We propose to implement a Variable Amplitude Module (VAM), a gearbox mechanism that allows for reciprocating sinusoidal output of continuously variable amplitude to be generated using a single continuously-rotating prime mover (e.g. motor) together with a single control input. This is well suited to replicating the modulated reciprocating motion patterns found in Nature. The VAM will have a number of applications in biomimetics and legged robotics. As a demonstration of the capabilities of the VAM mechanism, we present here the Variable Amplitude Module Orthogonal Slider (VAMOS). The VAMOS, Fig. 1, is a hexapedal robot featuring one prime mover and one servo (control input) that is capable of turning with arbitrary curvature, from walking in a straight line to turning on the spot.

II. RELATED WORK

There are a number of different approaches to robotic locomotion in the literature, with great variation in complexity,

size, functionality and how closely the biological counterpart is mimicked.

Hydraulic and pneumatic actuators have high power density and high force output, allowing for joints to be driven directly. Hydraulic actuation is implemented in the Big Dog robot [7] and other similar large and powerful robots. While the performance of such robots is generally superior at larger scales, the mechanical complexity, unfavourable scaling of fluid flow losses and the requirement of active valves for each independent make such actuation systems generally less suited for smaller or low cost robots.

Electric motors are a more accessible actuation technology. A commonly adopted approach is to use one motor per joint (e.g. [8], [10], allowing for each joint to be controlled independently so that arbitrary gaits and motions can be generated. However, the angle of each joint must be directly set by the central controller. Multiple actuators will generally result in greater complexity and higher cost. Moreover, actuators directly driving joints will generally be required to withstand high torques, necessitating high gear ratios which adversely affect efficiency. For every gait cycle, each motor must be accelerated and decelerated which further reduces efficiency.

Rather than controlling each muscle independently, Nature frequently employs the principle of Embodied Intelligence for generating gaits [11]. Here, the brain (central controller) controls the motion at a higher level and the low-level control signals are generated by reflexes and from the dynamics of the motion. Thus, very little control effort is required to produce gaits that are energy efficient and robust to perturbations. In a similar manner, it is desirable to create robots that do not rely on complex driving signals from the central controller for locomotion.

In the other extreme, Coros et al [12] present a framework for creating mechanical animatronic characters with arbitrary gait-like patterns resulting from a single continuously-driven rotating input. Here, the generation of the gait is devolved from the central controller to the body of the robot, encoded through its kinematic structure. The gait of each character is fixed, with each limb following a predefined trajectory, so this framework is not directly applicable to robotic applications where control is required for gait adjustment such as turning.

Optimal robotic locomotion systems can be sought by combining both design approaches, where some aspects of the gait is devolved to the mechanical structure of the robot but the higher-level gait pattern can still be controlled.

The Dash robot [13], inspired by the cockroach, is the fastest walking robot when measured in body-lengths per second. This employs a single prime mover, with the trajectory of each leg being generated mechanically. A control input changes the relative step lengths of the left and right side by deforming the compliant frame of the robot, to enable turning.

Similarly, the Sprawl series of hexapedal robots [6], [14] feature a single prime mover rotating continuously, with the motion of each leg being generated mechanically and servomotors varying the angle of each leg in order to achieve turning and control over the gait.

There are also legged robots employing ‘whegs’, i.e. legs that are rotated continuously at the ‘hip’ joint. Notably, the hexapedal RHex [15] can rapidly traverse steps and rough terrain. However, the continuously driven joints bear little resemblance to joints found in Nature. A more subtle shortcoming of this approach is that as the step length is fixed, and the phase between the motion of the legs must be fixed to ensure a stable gait[1], the turning radius cannot be varied continuously.

Our work here follows along the lines of the Dash and Sprawl robots, using a continuously-driven prime mover along with a control input. However, we expect the VAM mechanism presented here to be more readily transferable to other robotic locomotion applications, as a building block. Moreover, while both the Dash and Sprawl robots are insect-sized, the VAM will readily scale to larger and more powerful robots.

III. VARIABLE AMPLITUDE MODULE

The Variable Amplitude Module (VAM) is a mechanism that allows for reciprocating sinusoidal output of a continuously-variable amplitude to be generated from a constantly-rotating drive input together with a single control input. The control input is only varied to change the output amplitude. In robotic locomotion applications where an electric motor is used as the prime mover, the VAM's core advantage of a continuously-variable amplitude output is compounded by the fact that it allows the electric motor to be geared for maximum power or efficiency, and to always operate at the point of optimal efficiency. This is in contrast to the use of servo motors to directly drive joints. The VAM mechanism has been described in the literature [16, pp. 130–132], and used in flapping Micro Air Vehicles [17]. Here, we present a novel application of the VAM for legged robotic locomotion, along with a kinematic analysis of the VAM mechanism.

As implemented here, the VAM is based around a hypocycloid mechanism consisting of a planet attached to a carrier and meshing with an annulus gear, as shown in Fig. 2. The carrier is the main drive input, and the control input rotates the annulus. The gear ratio between the planet and annulus gear is 2:1, which means that if we drive the carrier then a point on the pitch circle diameter of the planet gear traces out a straight line across the diameter of the annulus. We attach an output pin to a point on the pitch circle diameter of the planet gear. With a Scotch yoke connected to this pin, this movement is then converted to a sinusoidal output. By rotating the annulus, we can change the orientation of the line traced out by the pin and thus vary the amplitude of the sinusoidal output as indicated in Fig. 3.

The VAM mechanism could also be implemented differently, depending on the specific application requirements. An alternative for the hypocycloid mechanism using only

[1]Not the case for wheeled robots with differential steering

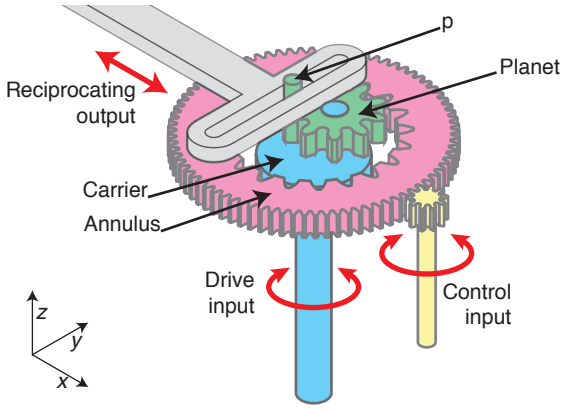

Fig. 2. Isometric drawing of the VAM. Annotated schematic drawing of the VAM. The carrier, in blue, is the main drive input, and the pink annulus is driven by the control input. As the carrier is driven, the point p on the pitch circle of the planet will trace out a straight line across the diameter of the annulus. With a Scotch yoke, we convert this to a reciprocating sinusoidal motion. Turning the annulus changes the orientation of the line traced out by p, thus changing the amplitude of the sinusoidal output.

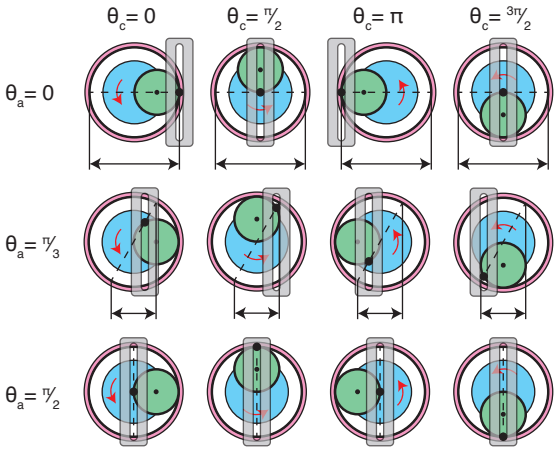

Fig. 3. Views of the Variable Amplitude Module (VAM) at 4 points in the cycle ($\theta_c = 0, \pi/2, \pi, 3\pi/2$, when running at full amplitude ($\theta_a = 0$), half amplitude ($\theta_a = 3\pi/2$) and zero amplitude ($\theta_a = \pi/2$). Meshing gears are shown as bold black lines.

external gears is presented in [16, p. 132], which produces a greater stroke relative to the size of the gears. The Scotch yoke could be approximated with a crank-rocker or crank-slider mechanism [18]. A crank-rocker mechanism would eliminate the need for prismatic joints. However, with both a crank-rocker and a crank-slider mechanism the output would no longer be sinusoidal and it would not be possible to reduce the output amplitude to zero. The mechanism could also be created without gears, by connecting the offset pin of the carrier to a Scotch yoke sliding on the annulus. By rotating the annulus, a point on this Scotch yoke would trace out a line across the diameter of the annulus equivalently to the hypocycloid mechanism. Again, it would be possible to approximate the behaviour of the Scotch yoke with a crank-rocker mechanism, to yield a mechanism with only revolute joints. The different possible implementations will present tradeoffs in terms of performance and complexity. The VAM implemented here, using a hypocycloid gear and Scotch yoke, is compact and relatively simple and produces a sinusoidal output where the amplitude can be reduced to zero.

The kinematics of the mechanism are derived in the following section.

A. Analysis

The Variable Amplitude Module (VAM) consists of a hypocycloidal gear mechanism, with a planet gear mounted on a carrier at point C and meshing with an annulus gear, as shown in Fig. 4. The gear ratio between the planet and annulus is 2:1. An output pin is attached to a point P on the pitch circle of the planet gear. Let us define the angle of rotation of the planet, annulus and carrier as θ_p, θ_a and θ_c respectively, as labelled in Fig. 4. Without loss of generality let the initial configuration of the unit be $\theta_p = \theta_a = \theta_c = 0$. Let us denote the diameter of the annular gear by $2A_0$, so that the radius of the planet gear is $A_0/2$.

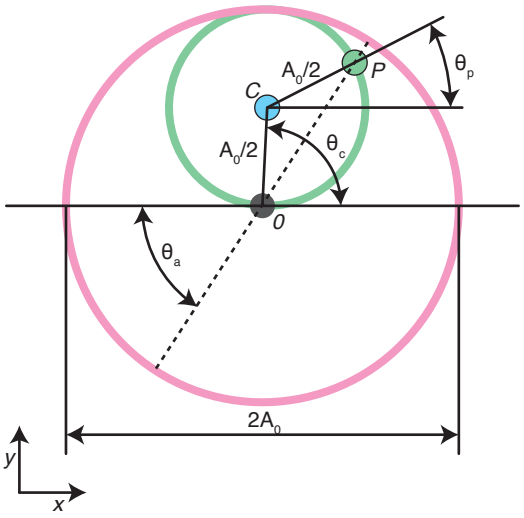

Fig. 4. Schematic drawing of the hypocycloid part of the VAM mechanims, with annotations. θ_a, θ_c and θ_p are the angles of the annulus, carrier and planet respectively. The diameter of the annulus is $2A_0$. The center of the planet is at point C (attached to the carrier), and the point P is attached to the Scotch yoke (not shown).

We wish to derive an expression for the position of the output pin p as a function of the inputs θ_a and θ_c. We can readily write down the kinematic relationship

$$\theta_p = 2\theta_a - \theta_c. \tag{1}$$

Now, consider the mechanism to lie in the complex plane. The position of point p is given by

$$\begin{aligned} p &= A_0\left(e^{j\theta_c} + e^{j\theta_p}\right) && (2)\\ &= A_0\left(e^{j\theta_c} + e^{j(2\theta_a-\theta_c))}\right) && (3)\\ &= A_0\left(e^{-j(\theta_a-\theta_c)}e^{j\theta_a} + e^{j(\theta_a-\theta_c)}e^{j\theta_a}\right) && (4)\\ &= A_0\cos\left(\theta_a-\theta_c\right)e^{j\theta_a} && (5)\end{aligned}$$

Consider the mechanism with a Scotch yoke free to move

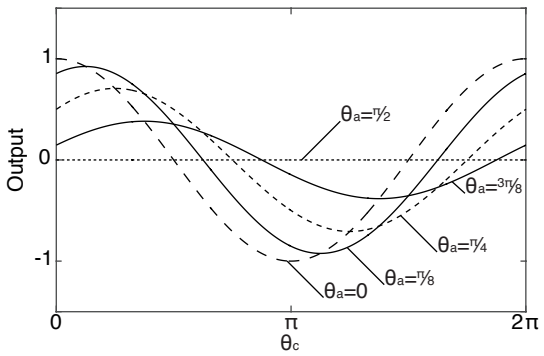

Fig. 5. Plot showing the output of the VAM for the same drive input, at different amplitudes. It can be seen that the phase changes when the amplitude is varied.

in the x-direction and taking out the real part of p. Then the output s is given by

$$s = A_0 \cos(\theta_a - \theta_c) \cos\theta_a \tag{6}$$

θ_c is the drive input, and θ_a is the control input. If we fix θ_a and drive θ_c at a constant angular velocity, then it is seen that s is a cosine function with amplitude $A_0 \cos\theta_a$ and phase shift θ_a.

Fig. 5 shows the output of the mechanism as θ_c is driven through a full rotation, for 5 different values of θ_a going from zero amplitude to full amplitude. This illustrates the coupling between amplitude and phase shift.

We believe the VAM is a building block that has a number of applications in robotics, both as presented above and as a starting point for modifications. The VAMOS robot presented here uses a modified two-output version of the VAM.

IV. VAMOS: A TWO-MOTOR HEXAPOD WITH ACKERMANN STEERING

To demonstrate the capabilities of the VAM, we present the VAMOS hexapedal robot. By exploiting the VAM, the VAMOS is capable of walking and turning with arbitrary curvature using a continuously-rotating prime mover and a single control input. This mode of control is similar to Ackermann steering as used on automobiles. The VAMOS features a VAM mechanism with two Scotch yokes at perpendicular orientations. As will be shown, this configuration allows for mixing between the two outputs. We use each output to control the step length of the left and right legs, respectively. By modulating the step length, we are able to turn while still maintaining synchronisation between the legs i.e. take the same number of steps.

A. Concept

The VAMOS (Fig. 1) is a hexapod robot with an alternating tripod gait. The dorsoventral (up-down) displacement of the legs is fixed, driven by a cam mechanism. For the rostrocaudal (back-front) displacement of the legs, the VAMOS implements a Variable Amplitude Model with two sliders, oriented at right angles. The sliders drive the movement of the left and right legs respectively. With the control input of the VAM, the relative step lengths of the left and right side can be varied to enable turning.

B. Design and fabrication

The VAMOS was fabricated mainly from laser-cut acetal plastic, with exception of the drive shafts. A primary concern has been ease of fabrication; we wanted to create a design that could be readily replicated with equipment typically available at universities, fab labs and maker spaces. This also presents a great contrast to robots such as Big Dog which feature very high mechanical complexity.

CAD drawings of the VAMOS are shown in Fig. 6, with the different mechanisms of the robot colour-coded. To aid re-use and modification of the VAMOS designs, the CAD files have been made open source and freely available on Github [link will be added for final version]. It is hoped that the VAM provides a platform that can be exploited in a wide range of robotic applications.

The fabricated VAMOS prototype is shown in Fig. 1. It is tethered, and uses a brushed DC motor with an 62:1 inline gearbox (Como Drills 944D621) as its prime mover and an RC servo (Hitec HS-5055MG) as the control input. The overall size of the robot is 180 mm long by 230 mm wide by 130 mm tall, and the mass is 405 g. The length of each leg, from hip joint to lower extremity, is 78 mm.

C. Analysis

Let us define a coordinate system as shown in Fig. 6, with the x-axis along the rostrocaudal (back-front) axis of the robot, the y-axis going from the left side to the right side and the z-axis along the dorsoventral (up-down) axis.

In the interest of clarity we will here present a simplified kinematic model of the VAMOS. We will assume that the rostrocaudal and dorsoventral mechanisms both are linear. The VAMOS has been designed so that in the neutral position the angle between connected links is as close as possible to $\pi/2$, making the assumption of linearity acceptable for small angles. We will also assume that each leg only moves in the x- and z-directions, with negligible movement in the y-direction. Each leg will thus trace out an ellipse in the $x-z$-plane.

The dorsoventral mechanism of the VAMOS is based around a cam, driven from the prime mover drive shaft, which drives a slider along the dorsoventral axis. Bell-crank mechanisms at alternating orientations create alternating dorsoventral movements for each of the leg, and ball-end links transfer the movements to the legs. Fig. 6 includes a view of the dorsoventral mechanism. Assuming that the mechanism is linear, and taking our inputs to the VAM to be θ_c and θ_a as before, the dorsoventral movement of the right front leg is then given by

$$z_{R1} = A_z \cos\theta_c,$$

where we use subscripts L and R and numbers 1–3 to denote the individual legs. With the alternating tripod gait,

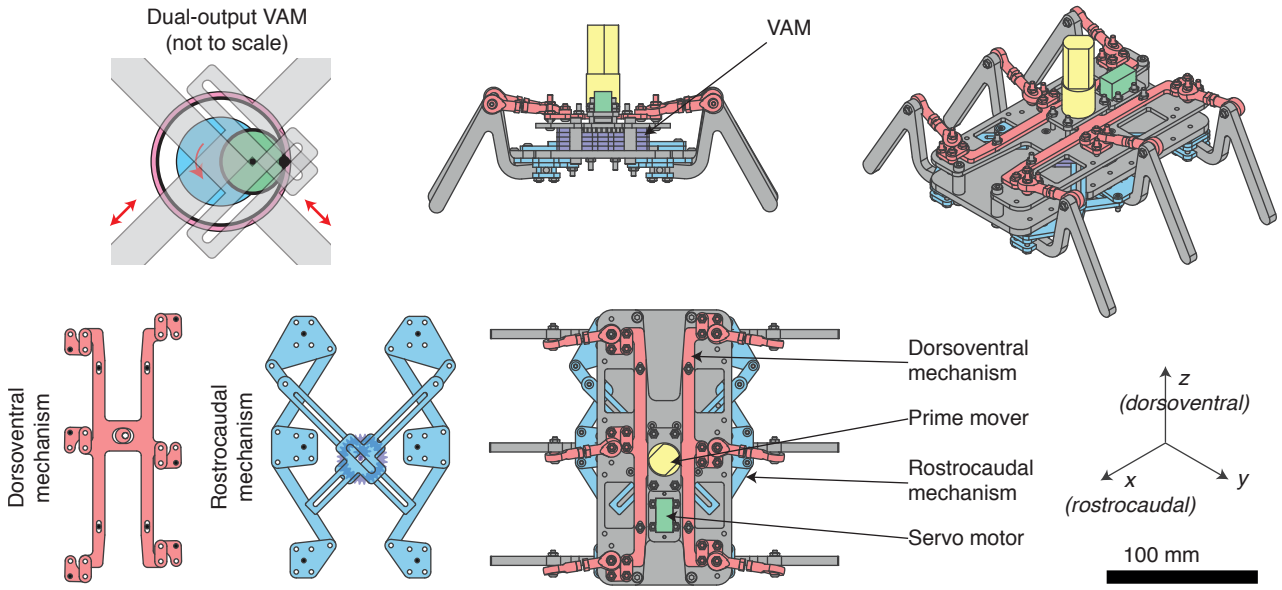

Fig. 6. CAD drawings of the VAMOS robot. Views showing the dorsoventral and rostrocaudal mechanisms in isolation have been included. A close-up schematic drawing of the dual-output VAM with two sliders oriented at right angles has been included, c.f. Fig. 3 (not to scale).

the relationship between the dorsoventral movements of all the legs is given by

$$z_{R1} = -z_{R2} = z_{R3} = -z_{L1} = z_{L2} = -z_{L3}.$$

For the VAMOS robot presented here, the dorsoventral amplitude A_z is 2.3 mm.

For the rostrocaudal mechanism, we utilise a single VAM with two sliders orthogonal to each other as shown in Fig. 6. Taking $\theta_a = 0$ to be along the positive x-axis, the slider driving the right legs moves along the line $y = -x$, or at an angle of $-\pi/4$, and the slider driving the left legs moves along the line $y = x$ or at an angle of $\pi/4$. As shown in Fig. 6 in blue, a link connects the output of the slider to the base of the front leg. The remaining legs are in turn driven by links from the base of front leg, as seen in the figure. Again, the mechanism has been designed so that in the neutral position the angle between connected links is $\pi/2$, so that for small angles the mechanism behaves linearly.

In this case, and again with the assumption of linearity, we can write the rostrocaudal position of the legs as

$$x_{R1} = A_x \cos(\theta_a - \theta_c) \cos\left(\theta_a + \frac{\pi}{4}\right) \quad (7)$$

and

$$x_{L1} = A_x \cos(\theta_a - \theta_c) \cos\left(\theta_a - \frac{\pi}{4}\right) \quad (8)$$

with the position of the remaining legs being given by

$$x_{R1} = -x_{R2} = x_{R3},$$

$$x_{L1} = -x_{L2} = x_{L3}.$$

The rostrocaudal amplitude A_x is 24 mm for the robot presented here.

Note that we have coupled the relative phases of the dorsoventral and rostrocaudal movements so that at $\theta_a = \pi/2$ the left and right step lengths are equal and the dorsoventral and rostrocaudal motions are $\pi/2$ out of phase as required for an alternating tripod gait. This means that at $\theta_a = \pi/2$ each leg will trace out an ellipse with the major axis aligned with the x-direction. This is optimal, as each leg lifts off and touches down at the extremal points.

As we begin to change θ_a away from $\pi/2$ in the positive direction, it can be seen from (7) and (8) that the amplitude of x_{R*} will increase while the amplitude of x_{L*} will decrease. This will cause the robot to turn. Changing θ_a will also result in a phase shift of x_{R*} and x_{L*}, with no change in z_{**}. As the rostrocaudal and dorsoventral movements will no longer be $\pi/2$ out of phase, the major axis of the ellipse traced out by each leg will no longer align with the x-direction. We have plotted the ellipse traced out by each leg for a set of different amplitudes in Fig. 7. As the major axis of the ellipse moves away from the x-axis, the effective step length (the step length while the leg is on the ground) decreases.

We can solve for the effective step length of the left and right legs as θ_a is varied, by setting $z_{**} = 0$. This allows us to plot the possible combinations of x_{R*} and x_{L*} that can be obtained as θ_a goes from 0 to π (the period is π rather than 2π as can be observed from (6)). This is depicted in Fig. 8.

Fig. 8 gives insight into the turning behaviour of VAMOS as θ_a is varied. At $\theta_a = \pi/2$, $x_{R*} = x_{L*}$ and the robot walks straight ahead. Increasing θ_a towards $5\pi/8$ causes an increase in x_{R*} and a decrease in x_{L*}, so the robot will turn towards the left with increasing curvature and with the overall forward speed of the robot being relatively constant. As θ_a increases further, towards $3\pi/4$, the curvature increases further while the overall forward speed of the robot decreases. At $\theta_a = 3\pi/4$, $x_{L*} = 0$ and therefore the left side of the robot is stationary. Further increasing θ_a towards

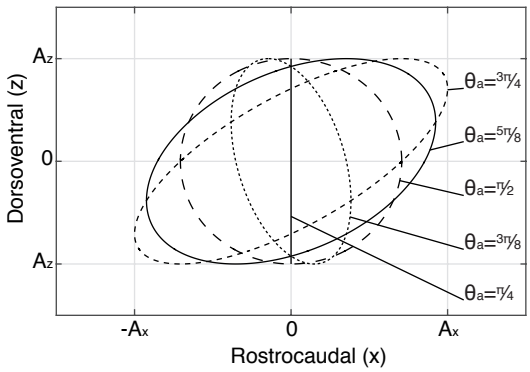

Fig. 7. Ellipses traced out by the right legs, as θ_a is varied. As θ_a changes, the major axis of the ellipse moves away from the x-axis, causing the effective step length to be decreased. For the left legs, the effect of θ_a is mirrored about $\theta_a = \pi/2$.

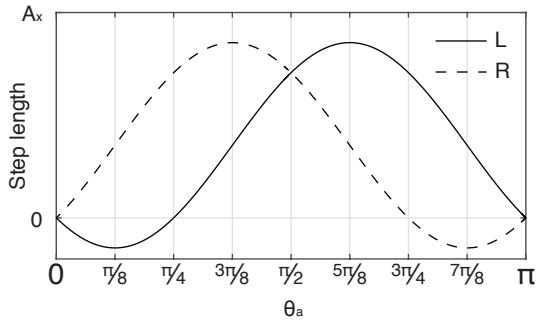

Fig. 8. Combinations of left (x_{L*}) and right (x_{R*}) step length as θ_a is varied.

π makes x_{L*} negative, meaning that the left side is stepping backwards while the right side is stepping forwards. This allows for turning with even greater curvature.

In order to turn on the spot, we require $x_{L1} = x_{R1}$ (because we have fixed $z_{R1} = -z_{L1}$). According to our analysis presented here, in the idealised case this will only occur at $\theta_a = \pi$ where $x_{L*} = x_{R*} = 0$ so that the robot is not technically able to turn on the spot. However, if we introduce a small deadband around the center point of the dorsoventral mechanism, which can be done by increasing tolerances during fabrication, the VAMOS robot is able to turn on the spot.

D. Evaluation

We have conducted an experiment in order to demonstrate the capability of the VAMOS to walk and turn with arbitrary curvature. We take curvature to mean the reciprocal of turning radius. The robot was set to walk for a fixed duration, for a range of different curvatures.

Experiments were carried out in an arena, where a single overhead camera tracked the robot using LED markers. The position and orientation of the robot was extracted from the video using a custom tracking implementation in MATLAB.

We picked a representative set of control inputs (θ_a) covering the space of possible turning curvatures. Each trial in our experiment shows a different θ_a, but with θ_a being held constant for the duration of the trial. With a fixed θ_a, we would expect the robot to walk along a trajectory with constant curvature.

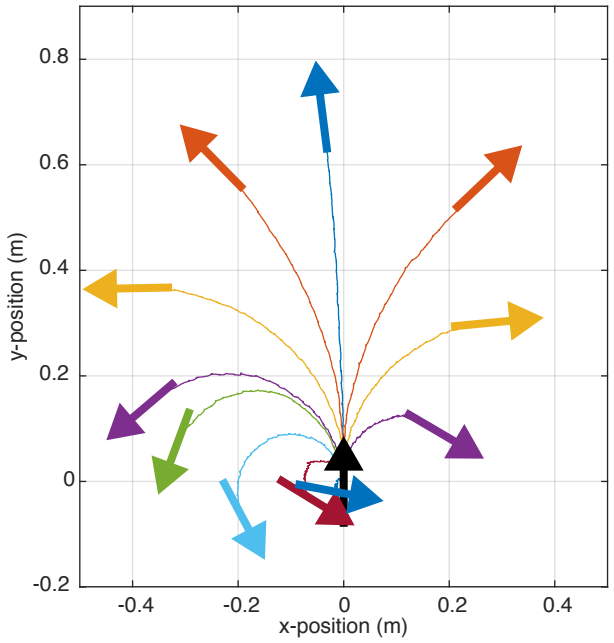

Fig. 9. VAMOS walking trajectories, with each line showing a trial with a different value of θ_a. We kept θ_a fixed through each trial. The black arrow indicates the starting location, and the coloured arrows show the final robot position. It can be seen that VAMOS is able to turn with arbitrary curvature, including turning on the spot.

For each trial the robot was placed at a known starting location and angle, and θ_a was set. The prime mover was then driven at a fixed speed for a fixed duration of 10 s, and the resulting trajectory was tracked.

Fig. 9 shows the resulting tracjectories. The initial position of the robot is shown by the black heavy arrow, with the arrowhead indicating the front of the robot. Each thin line indicates the trajectory of the centroid of the robot, with the coloured heavy arrows showing the position of the robot at the end of the 10 s trial.

It can be seen from the figure that the robot is capable of walking in turns with arbitrary curvature by varying θ_a. As each trial is for the same duration, we can also observe that the forward speed of the robot is greater when the curvature is small. This aligns with the previous analysis as presented in Fig. 8.

From the trajectories, we can determine the forward speed of the robot as well as the curvature. Fig. 10 plots forward speed against curvature, for the same trajectories presented in Fig. 9. The maximum forward speed is seen to be 0.077 m/s, or 0.43 BL/s (body lengths per second). As would be expected, the speed decreases with increasing curvature.

V. DISCUSSION

We have presented the VAMOS robot and the VAM module. The VAMOS robot is one possible application of the

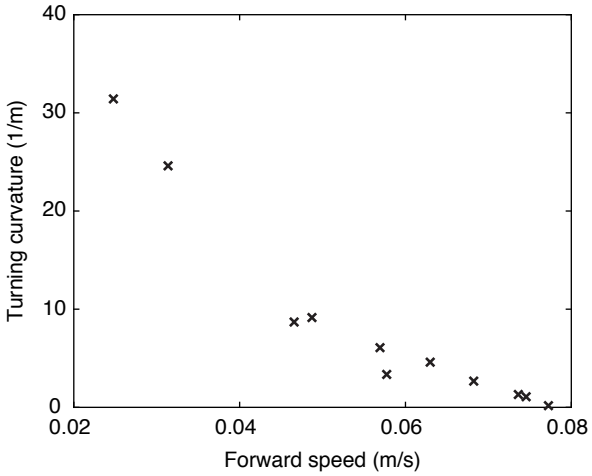

Fig. 10. Plot of forward speed against curvature (reciprocal of turning radius) for the trajectories shown in Fig. 9. The maximum forward speed is 0.077 m/s, or 0.43 BL/s (body lengths per second).

VAM, but the VAM could also be readily adapted to other robotics applications. Any application requiring amplitude control of a sinusoidal output, which includes most examples of animal locomotion, is a possible application.

The VAMOS robot presents an easy-to-use platform for basic legged robotic locomotion, that could readily be used in place of a differential drive system or Ackerman steering. It could also readily be adapted to suit different purposes. Here we have used mechanical linkages to drive the legs. It would also be possible to combine the VAM with a cable-driven linkage as used in the Sprawl robots [6], [14], allowing for even greater flexibility.

An interesting feature of the VAMOS robot is that we require continuous rotation of the prime mover, with no demand for position control. As such, it would not be infeasible to drive this with a combustion engine. This could allow for simple and low-cost, easy-to-control robots with high power.

There could also be exciting opportunities in combining the computational design tool for single-motor mechanical characters presented in [12] with the VAM module, to enable linkage-based characters and robots for walking and turning.

VI. CONCLUSIONS

We have introduced the VAM mechanism for legged robotic locomotion, and presented a kinematic analysis. The VAM creates a sinusoidal output with continuously-variable amplitude from a continuously-rotating drive input and a single control input. Variable-amplitude reciprocating motions are seen in most locomotion mechanisms found in Nature, so this mechanism is expected to have many applications in biomimetic locomotion.

The VAMOS robot demonstrates the capabilities of the VAM to produce a sinusoidal output of variable amplitude for hexapedal locomotion. The variable amplitude is exploited through the use of a novel orthogonal drive mechanism that enables the stride length of left and right legs to be modulated for turning from a single control actuator. The presented VAMOS prototype is fabricated almost exclusively by laser cutting, and the design files for both the VAMOS and the VAM have been made available on Github [link to be added for final version].

It is our hope that both the VAM and the VAMOS will become building blocks for robotic design that can readily be constructed, used, and modified to create a new generation of simple biomimetic walking, running and swimming robots.

ACKNOWLEDGEMENTS

The authors would like to thank the anonymous reviewers for helpful comments, and for pointing out the double-Scotch-yoke mechanism as an alternative to the hypocycloid gears.

REFERENCES

[1] M. H. Dickinson, "How Animals Move: An Integrative View," *Science*, vol. 288, no. 5463, pp. 100–106, Apr 2000.
[2] A. J. Ijspeert, "Biorobotics: Using robots to emulate and investigate agile locomotion," *Science*, vol. 346, no. 6206, pp. 196–203, 2014.
[3] K. Y. Ma, P. Chirarattananon, S. B. Fuller, and R. J. Wood, "Controlled flight of a biologically inspired, insect-scale robot," *Science*, vol. 340, no. 6132, pp. 603–607, 2013.
[4] O. C. D. Marchese, Andrew D. and R. Daniela, "Autonomous soft robotic fish capable of escape maneuvers using fluidic elastomer actuators," *Soft Robotics*, vol. 1, 2014.
[5] S.-M. Song and K. J. Waldron, *Machines that walk: the adaptive suspension vehicle*. MIT press, 1989.
[6] A. J. Mcclung, M. R. Cutkosky, and J. G. Cham, "Rapid Maneuvering of a Biologically Inspired Hexapedal Robot," *Proc IMECE04, Anaheim, CA, USA*, 2004.
[7] M. Raibert, K. Blankespoor, G. Nelson, R. Playter, and T. B. Team, "BigDog, the rough-terrain quadruped robot," in *IFAC Proceedings Volumes, Seoul, Korea*, vol. 17, no. 1 PART 1, 2008, pp. 6–9.
[8] M. Hutter, C. Gehring, M. Bloesch, M. A. Hoepflinger, C. D. Remy, and R. Siegwart, "Starleth: A compliant quadrupedal robot for fast, efficient, and versatile locomotion," in *CLAWAR 2012, Baltimore, MD, USA*, 2012.
[9] C. S. Haines, M. D. Lima, N. Li, G. M. Spinks, J. Foroughi, J. D. Madden, S. H. Kim, S. Fang, M. J. de Andrade, F. Göktepe, *et al.*, "Artificial muscles from fishing line and sewing thread," *Science*, vol. 343, no. 6173, pp. 868–872, 2014.
[10] S. Rutishauser, A. Sprowitz, L. Righetti, and A. J. Ijspeert, "Passive compliant quadruped robot using central pattern generators for locomotion control," in *IEEE RAS-EMBS BioRob 2008, Scottsdale, AZ, USA*, 2008, pp. 710–715.
[11] R. Pfeifer, M. Lungarella, and F. Iida, "Self-organization, embodiment, and biologically inspired robotics," *Science*, vol. 318, no. 5853, pp. 1088–1093, 2007.
[12] S. Coros, B. Thomaszewski, G. Noris, S. Sueda, M. Forberg, R. W. Sumner, W. Matusik, and B. Bickel, "Computational Design of Mechanical Characters," *ACM Transactions on Graphics*, vol. 32, no. 4, pp. 83:1–83:12, 2013.
[13] P. Birkmeyer, K. Peterson, and R. S. Fearing, "DASH: A dynamic 16g hexapedal robot," in *IEEE/RSJ IROS 2009, St. Louis, MO, USA*, 2009, pp. 2683–2689.
[14] S. Kim, J. E. Clark, and M. R. Cutkosky, "ISprawl: Design and tuning for high-speed autonomous open-loop running," *International Journal of Robotics Research*, vol. 25, no. 9, pp. 903–912, 2006.
[15] U. Saranli, "RHex: A Simple and Highly Mobile Hexapod Robot," *The International Journal of Robotics Research*, vol. 20, pp. 616–631, 2001.
[16] N. Sclater and N. P. Chironis, *Mechansims and Mechanical Devices Sourcebook*, 4th ed. McGraw Hill, 2007.
[17] J. Ratti, E. Jones, and G. Vachtsevanos, "Fixed frequency, variable amplitude (fifva) actuation systems for micro aerial vehicles," in *IEEE ICRA 2011, Shanghai, China*, 2011, pp. 165–171.
[18] G. Figliolini, M. Conte, and P. Rea, "Algebraic algorithm for the kinematic analysis of slider-crank/rocker mechanisms," *Journal of Mechanisms and Robotics*, vol. 4, no. 1, p. 011003, 2012.